MODIS Solar Reflective Band Calibration Algorithm Implementation

MCST Ref. No. G005

December 15, 1995

R. E. Veiga / GSC
H. E. Montgomery / NASA GSFC
M. D. Jones / GSC

MODIS Characterization Support Team

Acronyms and Abbreviations

A/D	Analog to Digital
A&E	Activation and Evaluation
AU	Astronomical Unit
BRF	Bidirectional Reflectance Factor
BRDF	Bidirectional Reflectance Distribution Function
ECI	Earth Centered Inertial
EV	Earth View
L1A	Level 1A
L1B	Level 1B
LUT	Lookup Table
MODIS	Moderate Resolution Imaging Spectroradiometer
OBC	On-Board Calibrator
SBRC	Santa Barbara Research Center
SDP	Science Data Production
SD	Solar Diffuser
SDSM	Solar Diffuser Stability Monitor
SV	Space View
TLCF	Team Leader's Computing Facility
TOA	Top of the Atmosphere

m	meter
μm	10^{-6} meter
s	second
ms	10^{-3} second
μs	10^{-6} second
sr	steradian
W	Watt

Introduction

Identification

This document describes the implementation of the Level 1B (L1B) algorithm for the calibration of the MODIS solar reflective bands. The L1B products are top-of-the atmosphere (TOA) Earth-scene pixel spectral radiance and bidirectional reflectance factor (BRF) and their corresponding uncertainties. In addition Space View (SV) statistics are an output product. A companion document entitled MODIS Solar Reflective Band Calibration Algorithm contains the reflective band calibration theory from which the algorithm contained herein is derived. The contributing authors of this document are

1. R. Veiga (veiga@gsfc.nasa.gov)
2. H. Montgomery (hmontgom@highwire.gsfc.nasa.gov)
3. M. Jones (mikej@ highwire.gsfc.nasa.gov).

Overview

The solar reflective band calibration algorithm provides estimates of the Earth-scene radiance and BRF for each pixel sampled by the MODIS bands 1-19, and 26. The MODIS scan mirror sweeps across an angular range from -55° to 55° relative to nadir. At nadir the along-track (direction of satellite travel) distance sampled in one scan is 10 km, while the width of the scan projected onto the Earth's surface is 2330 km. The projection of each detector's surface area onto the Earth's surface at nadir is a square region sampled at three spatial resolutions: 250 m, 500 m , and 1000 m, at sampling intervals of 83 μs, 167 μs, and 333 μs, respectively. These areas and sampling intervals define the MODIS pixels. TOA radiance entering the MODIS aperture is spectrally filtered, routed to the focal planes, and stimulates detector response.

The solar reflective band radiance calibration consists of determining the proportionality between detector output and radiance input from the SD, and in maintaining an accurate calibration for each detector. The SD is characterized in the prelaunch environment in order that its radiance can be calculated from the solar geometry occurring in-orbit. The stability of the SD is maintained with the Solar Diffuser Stability Monitor (SDSM).

Applicable Documents

1. MODIS Level 1B Algorithm Theoretical Basis Document 1995, B. Guenther, P. Abel, J. Barker, W. Barnes, H. Montgomery, R. Barbieri, M. Hopkins, M. Jones, D. Knowles, S. Qiu, S. Sinkfield, R. Veiga, N. Che, L. Goldberg, M. Maxwell, T. Zukowski, J. Baden, E. Knight, A. McKay, K.

Parker, and G. Godden, 1995.
2. MODIS Solar Reflective Band Calibration Algorithm, R. Veiga, H. Montgomery, and M. Jones, MCST Ref. No. G004, 1995.
3. Software Requirements Specification for the MODIS Level 1B Software System, P200-CD-001-001, MCST, June 15, 1995.
4. SDP Toolkit 4 Users Guide for the ECS Project, 333-CD-002-002, EOSDIS Core System Project, 1995.

Publications

Dixon, W. J., Ratios involving extreme values, *Ann. Math. Statist.*, 22, 68-78, 1951.

Jones, M. D., Algorithm description for applying the reflected band calibration, MCST memorandum, October 4, 1995.

Paltridge, G. W., and C. M. R. Platt, Radiative Processes in Meteorology and Climatology, Elsevier Scientific Publishing Co., 1976.

Seber, G. A. F., Linear Regression Analysis, Wiley, 1977.

SBRC-151868, Requirements for Ambient Calibration and Testing (AC) Support Software, App. A, SBRC, 1993.

Wehrli, C., Extraterrestrial Solar Spectrum, World Climate research Programme, Publication Series No. 7, WMO ITD-No. 149, pp 119-126, October, 1986

1 SD/SDSM Calibration System Description

Data from heritage instruments indicate that the output of photodetectors can change during long-term exposure to the space environment. In order to characterize this expected degradation, MODIS has been designed with several on-board calibration (OBC) subsystems.

1.1 Science Objectives and Design Overview

Part of the requirements for the Level 1B (L1B) calibration are that estimates of the following four quantities be produced for every detector sampling the Earth scene in the solar reflective bands: radiance, radiance uncertainty, BRF, and BRF uncertainty. The MODIS reflective bands are 1-19, and 26, with a total of 330 detectors. The detectors in the solar reflective spectral range are of the photovoltaic type, and have the property that the detector current varies linearly with irradiance. Thus all the calibration equations for these bands are linear equations, with each equation requiring a minimum of two calibration points for complete specification.

Both the radiance and BRF calibration depend on measurements made by each detector on the SD and the SV. The SD serves as a well-characterized, stable solar-reflective radiance source, while the SV provides the “zero-level” radiance for detector offset correction. Uncertainty in the radiance calibration is dependent on the accuracy of the prelaunch calibration. This uncertainty effectively becomes uncertainty in the value of the solar irradiance which is needed for subsequent calibrations with the SD. In order to maintain the stability of the SD the MODIS design incorporates the SDSM, a subsystem used for estimating the expected degradation of the SD BRF.

The reflectance calibration is based on the prelaunch-measured BRF of the SD, and is independent on the solar irradiance. Consequently the Earth scene BRF measurement is expected to have less uncertainty than the Earth scene radiance measurement which depends on an accurate prelaunch radiance calibration.

The land, ocean, and atmospheric science requirements from MODIS demand that the detectors in each band produce useful radiance estimates in specific ranges. The detector responsivities vary significantly from band-to-band, and to prevent detector saturation during solar calibration periods an attenuation screen must be used to reduce the SD irradiance reaching certain detectors. Thus during SD calibration periods, the SD screen can be either up (no solar attenuation) or down (solar attenuation). All bands can be calibrated when the screen is down, and all bands except 8-16 can be calibrated with the screen up. The maximum and typical radiance levels expected in each band from the earth scene are shown in Table 1.1 along with the radiance levels of the SD for a nominal solar incidence angle of 58°. The column in Table 1.1 headed by “N_D” is the number of detectors in the band. For bands 13 and 14, the time delay integration bands, a separate set of responsivities will be computed at each detector’s location.

The SD radiance levels in Table 1.1 were computed from integration of the solar spectrum measurements of Neckel and Labs [1984] weighted by the MODIS band relative spectral response. The in-flight values of solar irradiance will be measured by the instrument based on the prelaunch calibration, and there will be differences with those in Table 1.1. Accurate values for the SD radiance in-flight are critical to producing accurate earth-scene radiances, however the solar irradiances based on measurements external to MODIS are needed for quality control diagnostics. The TDI bands 13 and 14, shown schematically in Figure 1, operate with two arrays of detectors per band. One set operating in high-gain mode, and the other on low-gain mode. Processing must consider each mode as equivalent to a band.

Table 1.1
MODIS Design Radiance Levels by Band

Band	Screen U/D	SD L_{max} (screen up)	SD L_{max} (screen down)	Earth L_{max}	Earth L_{typ}	N_D
1	U	274.9[1]	23.4	685.0	21.8	40
2	U	169.3	14.4	285.0	24.7	40
3	U	336.5	28.6	593.0	35.3	20
4	U	320.5	27.2	518.0	29.0	20
5	U	80.5	6.8	110.0	5.4	20
6	U	39.8	3.4	70.0	7.3	20
7	U	14.7	1.2	22.0	1.0	20
8	D	304.5	25.9	175.0	44.9	10
9	D	328.1	27.9	133.0	41.9	10
10	D	316.3	26.9	101.0	32.1	10
11	D	330.6	28.1	82.0	27.9	10
12	D	314.6	26.7	64.0	21.0	10
13[2]	D	259.8	22.1	32.0	9.5	10,10
14[2]	D	253.9	21.6	31.0	8.7	10,10
15	D	215.1	18.3	26.0	10.2	10
16	D	163.1	13.9	16.0	6.2	10
17	U	150.6	12.8	185.0	10.0	10
18	U	136.6	11.6	256.0	3.6	10
19	U	135.6	11.5	189.0	15.0	10
26	U	62.2	5.3	89.9	6.0	10

[1]Radiance units are [W m^{-2} sr^{-1} μm^{-1}]. [2]Bands 13 and 14 operate in both of two gain states.

The SD system has been designed for solar irradiance to illuminate the SD for a period of approximately 2 minutes once per orbit near the North Pole for the AM platform. The sub-satellite latitude during SD illumination periods ranges from 40° during the summer solstice to 80° during the winter solstice. During the calibration period the solar incidence angle on the SD is centered near 58° , and changes by approximately 8° during the 2 minute period.

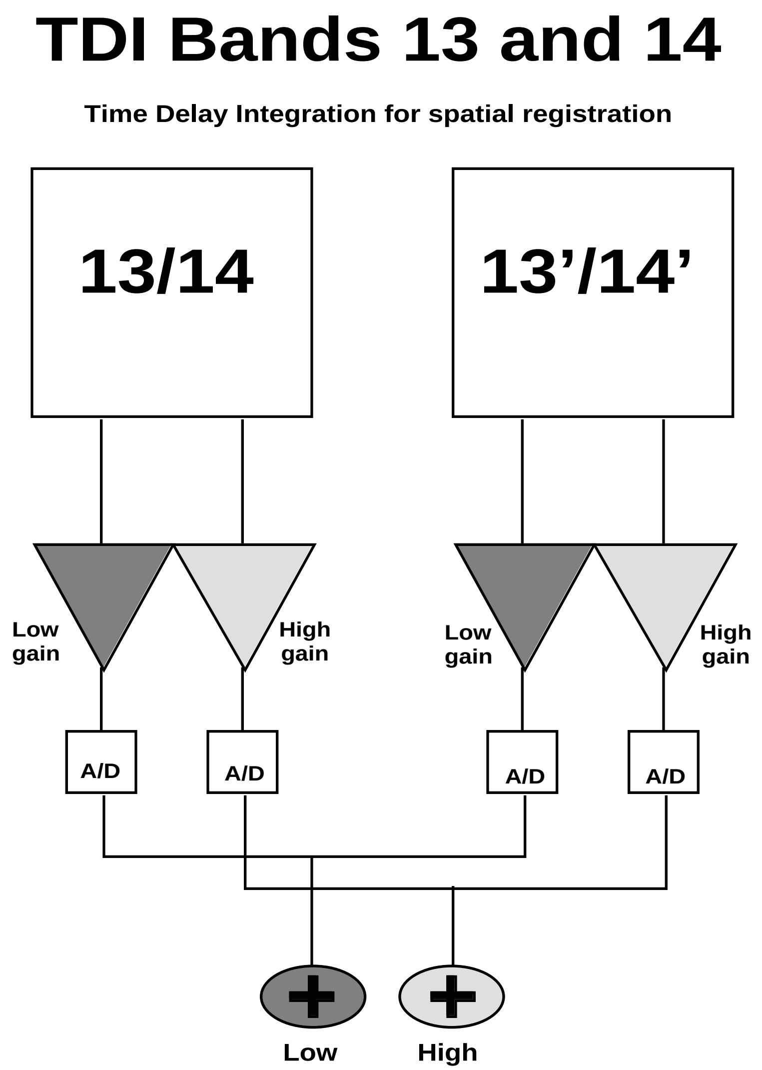

Figure 1. The TDI bands sum the outputs of two physically separate detector arrays in two different gain states.

During Activation & Evaluation (A&E), a period of time lasting for approximately 3 months, the SD will be used for performing system characterization. During operational processing the SD will be deployed as frequently as once per week up to once per month for radiance calibration.

Table 1.2 presents the scan mirror object space angles for the MODIS viewports relevant to calibration. The object space of the MODIS scan mirror begins at nadir where the scan angle is 0°. The first OBC encountered is the SD in a 2.5° sector. The object space scan time of 1.47717 s combined with 333.333 μs for the A/D digitization time yields 30.8 samples from the SD. Two other digitizing times (166.667 and 83.3333 μs) yield correspondingly larger sample sizes. The other sectors pertinent to calibration are shown in Table 1.2 along with their data volumes [SBRC-151868, 1993]. A maximum of 30 samples could be taken from the SD at the lowest sampling rate. However, the center 15 could be used in routine operation in order to minimize edge effects. SV samples are used every scan for detector offset correction with a maximum of 16 samples at the lowest sampling rate.

The SDSM operates asynchronously relative to the object space sampling depicted in Table 1.2, and it completes one scan cycle in 6 seconds. The SDSM has a 3-position fold mirror with the following sampling sequence: (1) sun, (2) zero-reference, (3) SD, and (4) zero-reference. Three samples are taken at each of the four locations. The SDSM cycle is repeated throughout the duration of the SD illumination period.

Table 1.2
Object Space Angles of MODIS View Ports

View Port	Start Angle	Stop Angle	Angle Difference	Samples at 333.333μs
SD	182.250°	184.750°	2.500°	30.8
SD to SRCA			22.547°	277.5
SRCA	207.297°	207.703°	0.406°	5.0
SRCA to BB			23.047°	283.7
BB	230.750°	232.050°	1.300°	16.0
BB to SV			28.850°	355.1
SV	260.900°	262.250°	1.350°	16.6
SV to Earth			42.750°	526.2
Earth	-55.000°	55.000°	110.000°	1354.1
Earth to SD			127.250°	1566.4
Total				4431.5

The SDSM bands' spectral transmittance are defined by a set of witness filters used during the manufacture of the MODIS focal planes. The wavelengths and bandwidths of the SDSM bands are listed in Table 1.3, and are simply the MODIS center wavelengths for 9 bands.

Table 1.3
SDSM Detector Filter Parameters

SDSM Band #	MODIS Band #	λ (nm)	Δλ (nm)
1	8	412	15
2	3	469	20
3	11	531	10
4	4	555	20
5	1	645	50
6	15	748	10
7	2	858	35
8	17	905	30
9	19	940	50

1.2 Correction of Detector Counts for Systematic Effects

Detector counts at the MODIS focal planes can be affected by focal plane temperature, scan mirror reflectivity differences between the two mirror sides, scan angle reflectivity variability on a given mirror side, and detector A/D linearity. Discussion of these effects is contained in Guenther et al. [1995], and the algorithm for correcting these effects is provided by Jones [1995]. All the solar reflective band detector count values measured at the MODIS focal planes used in the algorithm described in Sections 2-8 are the "effective" counts described in Jones [1995].

Part of the solar reflective band calibration algorithm is the calculation of mirror side reflectivity differences between the MODIS scan mirror sides, and the estimates of this quantity must be made available to other components of L1B.

1.3 Notation and Nomenclature

The primary purpose of L1B is to produce radiance and BRF estimates for each MODIS EV pixel, and to maintain an accurate radiometric calibration for each detector. The calibration depends on each detector's responsivity.

The term "reflectance" is used freely in reference to the SD or a property of the earth scene. In Sections 6 and 8 the EV BRF is calculated. The precise meaning of the scene reflectance is the scene bidirectional reflectance factor (BRF) a unitless quantity. When used in reference to the SD, the term "reflectance" refers to the SD BRDF.

Variables named "DN" or "CN" are used for digitized count data from the MODIS detectors or the SDSM detectors, respectively. Since MODIS uses 12 bit A/D converters the values in these types of arrays will range between 0 and 4095 counts.

Many arrays are used in the processing. Array indices are assumed to be non-zero positive integers. Instances where the symbol "*" is used as an index denotes all the data values contained within the array's indicated dimension.

The variable "B" is used to denote the band, and the normal counting sequence is most convenient for ordering, with the exception that band 26 processing occurs for B=20. However bands 13 and 14 each produce two separate outputs, and thus the band count climbs to 22 "bands". Presumably the code design will handle these anomalies. The description contained herein will proceed to describe arrays and indexing in Fortran style.

The variable “D” is used to denote the detector number within a band. Table 1.1 shows the number of detectors in each band. Array processing of specific bands uses the variable $N_D(B)$ to denote the range of D within the band B.

The variable “M” is used to denote the mirror side, and the two values M=1 and M=2 are used. The mirror side will be known from the Level 1A data stream.

The variable “S” is used to denote the scan for a given mirror side (M). The current scan is defined to be that scan occurring immediately after a given Earth View (EV) scan. It takes 1.47717 s for a given mirror side to complete 1 rotation.

Each section contains tables (if applicable) listing the names of array indices, data arrays, L1B control parameters, and external tabulated data and lookup tables (LUT).

Operational Processing

Two types of processing are implicit in this algorithm. The term *operational* shall refer to the operations executed for SV and calibration operations. SV operations include sampling the SV scan data, computing SV statistics, filtering SV data, and updating the SV buffer. Calibration operations include computing responsivity predictions, EV radiances, EV radiance uncertainties, EV BRF, and EV BRF uncertainties.

Solar Calibration Processing

The term *solar calibration* shall refer to the operations which must be executed whenever SD and SDSM data are available for radiance and BRF calibration. Execution of solar calibration processing occurs infrequently relative to operational processing.

2 Process SV Scans

SV data are needed continuously for detector offset correction. Thus this section of the L1B algorithm is part of the operational processing, whereas the algorithm described in Sections 3-7 are executed only during solar calibration periods when the SD is illuminated.

During solar calibration periods various quantities are updated as part of the calibration process. One of these is the relative reflectivity of the two scan mirror sides. In order to estimate this reflectivity ratio measurements must be segregated by mirror side. Thus all the data arrays used in this section contain an index (M) for mirror side.

Table 2.1
SV Array Indexing

Variable	Description	Range
B	Band index. Solar reflective bands: 1-19, 26.	1:20
D	Detector.	$1:N_D(B)$[1]
M	Mirror side.	1:2
S	SV scan.	1:SV_B_SIZE
F	SV sample.	1:60 bands 1-2 1:30 bands 3-7 1:15 bands 8-19,26

[1]See Table 1.1

Table 2.2
SV Variable Definition

Variable	Description
$DN_{SV}(B,D,M,F)$	SV scan data. SV scan vector has B, D, and M fixed.
$\overline{DN}_{SV}(B,D,M,S)$	SV scan vector average for scan S.
$N_{SV}(B,D,M,S)$	Number of SV samples for SV scan S (≤ 15, 30, or 60).
$S_{SV}(B,D,M,S)$	SV scan vector standard deviation for scan S.
SV_MIN(B,D,M)	SV scan vector minimum before filtering.
SV_MAX(B,D,M)	SV scan vector maximum before filtering.
$MN_{SV}(B,D,M,S)$	Minimum SV scan vector value for scan S.
$MX_{SV}(B,D,M,S)$	Maximum SV scan vector value for scan S.
$DN_0(B,D,M)$	SV buffer. Running average of SV scan vectors.
$K_0(B,D,M)$	Number of elements in all SV scan vectors of SV buffer.
$S_0(B,D,M)$	Standard deviation of SV scan vectors in SV buffer.
$MN_0^0(B,D,M)$	Minimum SV buffer value.
$MX_0^0(B,D,M)$	Maximum SV buffer value.
$MN_0^1(B,D,M)$	Minimum SV buffer value with $MN_0^0(B,D,M)$ removed.
$MX_0^1(B,D,M)$	Maximum SV buffer value with $MX_0^0(B,D,M)$ removed.
NUM_REJECT	Number of SV points rejected as outliers in a scan.

Table 2.3
SV Control Parameters

Parameter	Description
SV_B_SIZE	Number of scans in the SV buffer.
MAX_REJECT	Largest number of outliers rejected in SV count vector.
FSV	SV sector starting sample number ($FSV + N_{SV} \leq 15, 30, 60$).
DN_REJECT_LEVEL	Count data outlier test level for R10_TABLE table.

Table 2.4
SV Data Tables

Table	Description
R10_TABLE	Critical points of Dixon's R10 statistic.

The SV scan vectors reside in the array $DN_{SV}(B,D,M,*)$. These data represent the detector counts retrieved as the MODIS scan mirror sweeps across the SV once. Since there are a maximum of 16 samples at the 333.333 μs sampling period in the SV, the data for one SV scan represents a 5.3 ms period of time.

The SV buffer does not contain individual SV count data, but only statistics computed from the SV scan vectors for SV_B_SIZE scans of the SV, since the ultimate use of the SV buffer is for detector offset correction. The SV buffer contains SV scan statistics computed from the set of SV scans centered at the time of the current SV scan vector.

As the MODIS mirror rotates from one scan to the next, the oldest SV buffer elements are shifted out, and the statistics from the next future scan are shifted in. A circular index would be the optimal method for SV buffer pointing. The equations below use the index S to denotes the SV buffer elements. Successful implementation of the SV buffer across granules depends on the availability of previous and future granules. If a temporally contiguous SV buffer cannot be maintained, then the only option is to initialize a new SV buffer for each granule.

An illustration of the processing needed to compute SV buffer statistics from the SV scans is illustrated below as the MODIS mirror rotates twice (2 scans) for a given mirror side. The SV buffer's size is assumed to contain SV_B_SIZE = 5 elements. Reference to band and detector is omitted for clarity.

SV Scan Vector Statistics for Scan j of Mirror Side M

Scan	Count	Mean	Variance	Minimum	Maximum
j-2	N_{j-2}	U_{j-2}	V_{j-2}	$(MN)_{j-2}$	$(MX)_{j-2}$
j-1	N_{j-1}	U_{j-1}	V_{j-1}	$(MN)_{j-1}$	$(MX)_{j-1}$
j	N_{j}	U_{j}	V_{j}	$(MN)_{j}$	$(MX)_{j}$
j+1	N_{j+1}	U_{j+1}	V_{j+1}	$(MN)_{j+1}$	$(MX)_{j+1}$
j+2	N_{j+2}	U_{j+2}	V_{j+2}	$(MN)_{j+2}$	$(MX)_{j+2}$

SV Buffer Statistics for Scan j of Mirror Side M

Mean	$\dfrac{\sum_{i=-2}^{2} N_{j-i}U_{j-i}}{\sum_{i=-2}^{2} N_{j-i}}$
Total Count	$K_j = \sum_{i=-2}^{2} N_{j-i}$
Variance	$\dfrac{\sum_{i=-2}^{2}(N_{j-i}-1)V_{j-i} + K_j \sum_{i=-2}^{2} N_{j-i}U_{j-i}\left[(K_j - N_{j-i})U_{j-i} - 2\sum_{k>j-i}^{2} N_k U_k\right]}{K_j}$
Minimum	$\mathrm{Min}\left[(MN)_{j-2},(MN)_{j-1},(MN)_j,(MN)_{j+1},(MN)_{j+2}\right]$
Maximum	$\mathrm{Max}\left[(MX)_{j-2},(MX)_{j-1},(MX)_j,(MX)_{j+1},(MX)_{j+2}\right]$

On the subsequent scan the contents of the oldest SV vector is shifted out, and the contents of the next future SV vector is shifted in, and scan j+1 becomes the current scan.

SV Vector Statistics for Scan j+1 of Mirror Side M

Scan	**Count**	**Mean**	**Variance**	**Minimum**	**Maximum**
j-1	N_{j-1}	U_{j-1}	V_{j-1}	$(MN)_{j-1}$	$(MX)_{j-1}$
j	N_j	U_j	V_j	$(MN)_j$	$(MX)_j$
j+1	N_{j+1}	U_{j+1}	V_{j+1}	$(MN)_{j+1}$	$(MX)_{j+1}$
j+2	N_{j+2}	U_{j+2}	V_{j+2}	$(MN)_{j+2}$	$(MX)_{j+2}$
j+3	N_{j+3}	U_{j+3}	V_{j+3}	$(MN)_{j+3}$	$(MX)_{j+3}$

SV Buffer Statistics for Scan j+1 of Mirror Side M

Mean	$\dfrac{\sum_{i=-1}^{3} N_{j-i}U_{j-i}}{\sum_{i=-1}^{3} N_{j-i}}$
Total Count	$K_j = \sum_{i=-1}^{3} N_{j-i}$
Variance	$\dfrac{\sum_{i=-1}^{3}(N_{j-i}-1)V_{j-i} + K_j \sum_{i=-1}^{3} N_{j-i}U_{j-i}\left[(K_j - N_{j-i})U_{j-i} - 2\sum_{k>j-i+1}^{3} N_k U_k\right]}{K_j}$
Minimum	$\mathrm{Min}\left[(MN)_{j-1},(MN)_j,(MN)_{j+1},(MN)_{j+2},(MN)_{j+3}\right]$
Maximum	$\mathrm{Max}\left[(MX)_{j-1},(MX)_j,(MX)_{j+1},(MX)_{j+2},(MX)_{j+3}\right]$

2.1 Filter Extreme Values in the SV Scan Vector

Check each element of the current SV scan vector. When SV outliers are detected they are removed. An outlier may be caused by energetic particles in the SAA or polar horns, stray light, celestial bodies, or undetermined instrument transients. Analysis of engineering model data has shown that the normality assumption for count data in the SV scan is valid. The SV data remaining after the outlier detection algorithm has been applied will constitute the “filtered” SV data. The two-sided discordance test for an extreme outlier in a normal sample with unknown variance [Dixon, 1951] forms the basis for the rejection algorithm. The algorithm is described in the following steps, and must be applied to each detector.

If the name of the outlier rejection function is DN_FILTER, an example of its use in the context of SV processing along with the necessary input arrays and output data could be

$$\mathrm{DN\_FILTER}(\,DN_{SV}(B,D,M,*), MN_0^0(B,D,M), MN_0^1(B,D,M), MX_0^0(B,D,M), MX_0^1(B,D,M), K_0(B,D,M)\,)$$

where the ‘*’ denotes the filtering process is performed on all data residing in the corresponding dimension. The routine needs access to the table of critical points R10_TABLE, and the algorithm is described in Sections 2.1.2 and 2.2.3.

2.1.1 SV Scan Vector Minimum and Maximum Before Filtering

The two values, SV_MIN and SV_MAX, are the maximum and minimum of the input vector $DN_{SV}(B,D,M,*)$ before the filtering process is applied.

$$\mathrm{SV\_MIN}(B,D,M) = \mathrm{Min}\left[DN_{SV}(B,D,M,*)\right]$$
$$\mathrm{SV\_MAX}(B,D,M) = \mathrm{Max}\left[DN_{SV}(B,D,M,*)\right]$$

2.1.2 Test Statistic for Outliers

For clarity the following description does not show variables with their full names and indexing (B,D,M,S). The relevant count values and order statistics used here are computed in Sections 2.5, and 2.8, respectively.

Suppose the SV buffer consists of the values $X_1, X_2, ..., X_m$, and the current SV scan vector consists of the values $Y_1, Y_2, ..., Y_n$, where $n < m$. Let $X_{(1)}, X_{(2)}, ..., X_{(m)}$ and $Y_{(1)}, Y_{(2)}, ..., Y_{(n)}$ denote the order statistics of the SV buffer, and the current SV scan vector, respectively. The order statistics of the SV buffer have the property that

$$T_D^m = \max\left[\frac{X_{(m)} - X_{(m-1)}}{X_{(m)} - X_{(1)}}, \frac{X_{(2)} - X_{(1)}}{X_{(m)} - X_{(1)}}\right] < T_{D,\alpha}^m$$

where $\Pr[t > T_{D,\alpha}^m] = \alpha$ in Dixon's two-sided discordance test. The values of $T_{D,\alpha}^m$ are read from the table R10_TABLE. Nominal values for α are .05 and .01. R10_TABLE will contain the data for both values of α.

2.1.3 Test SV Scan Vector Elements for Inclusion in the SV Buffer

Find all values in the SV scan vector [$Y_{(1)}$, $Y_{(2)}$, ..., $Y_{(n)}$] which lie outside the interval of the SV buffer defined by $X_{(1)}<X< X_{(m)}$ (the search order should work from both extremes of the SV scan vector order statistics toward the median). Suppose $Y_{(i)}$ is such a value. Compute T_D^{m+1} as above using $Y_{(i)}$ either as the minimum or maximum. Reject $Y_{(i)}$ as an outlier if $T_D^{m+1} > T_{D,1-\alpha/2}^{m+1}$. If $Y_{(i)}$ is rejected increment the counter NUM_REJECT, and remove $Y_{(i)}$ from SV scan vector and decrement the SV count by one. Repeat this process for all other SV scan vector values outside the SV buffer range whenever NUM_REJECT<MAX_REJECT. If NUM_REJECT=MAX_REJECT the outlier search process stops and the remaining candidates of the SV scan vector which were not tested are accepted as valid data and retained in the SV scan vector.

2.2 SV Scan Vector Average

The filtered samples from one SV scan are averaged. During operational processing the SV is sampled every scan, independent of the state of SD illumination. SV processing should be suspended when the moon is in the SV, or spacecraft maneuvers are active. In this case SV statistics are held constant and used during all scans for which the moon is in the SV or maneuvers are being done.

$$\overline{DN}_{SV}(B,D,M,S) = \frac{1}{N_{SV}(B,D,M,S)} \sum_{F=FSV}^{F=FSV+N_{SV}(B,D,M,S)} DN_{SV}(B,D,M,F)$$

2.3 SV Scan Vector Variance

The filtered samples from one SV scan are used to compute the SV scan variance. The restrictions mentioned in Section 2.2 apply if the moon appears in the SV.

$$S_{SV}^2(B,D,M,S) = \frac{1}{N_{SV}(B,D,M,S) - 1} \sum_{F=FSV}^{F=FSV+N_{SV}(B,D,M,S)} \left\{ DN_{SV}(B,D,M,F) - \overline{DN}_{SV}(B,D,M,S) \right\}^2$$

2.4 SV Scan Vector Order Statistics

The filtered samples from one SV scan are used to compute the SV scan minimum and maximum. The restrictions mentioned in Section 2.2 if the moon appears in the SV.

$$MN_{SV}(B,D,M,S) = \min\left[DN_{SV}(B,D,M,F)\right]_{F=FSV}^{F=FSV+N_{SV}(B,D,M,S)}$$
$$MX_{SV}(B,D,M,S) = \max\left[DN_{SV}(B,D,M,F)\right]_{F=FSV}^{F=FSV+N_{SV}(B,D,M,S)}$$

2.5 SV Buffer Count

The number of data values implicit in the SV buffer is

$$K_0(B,D,M) = \sum_{S=1}^{SV\_B\_SIZE} N_{SV}(B,D,M,S)$$

2.6 SV Buffer Average

The running average of SV_B_SIZE SV scans is used in the detector offset correction process. It is computed from the SV buffer elements.

Processing	SV Buffer Average
Solar calibration	$DN_0(B,D,M) = \frac{\sum_{S=1}^{SV\_B\_SIZE} N_{SV}(B,D,M,S)\ \overline{DN}_{SV}(B,D,M,S)}{K_0(B,D,M)}$
Operational	$DN_0(B,D,1) = \frac{\sum_{M=1}^{2} \sum_{S=1}^{SV\_B\_SIZE} N_{SV}(B,D,M,S)\ \overline{DN}_{SV}(B,D,M,S)}{\sum_{M=1}^{2} K_0(B,D,M)}$

An incremental form for computing DN_0 would reduce processor loading as new SV scan statistics are shifted in and out of the SV buffer.

2.7 SV Buffer Standard Deviation

The standard deviation of the SV count buffer is a required output of L1B, and is computed as

Processing	SV Buffer Standard Deviation
Solar calibration	$S_0(B,D,M) = \sqrt{\frac{1}{K_0(B,D,M)}} \left\{ \sum_{S=1}^{SV\_B\_SIZE} (N_{SV}(B,D,M,S) - 1)\ S_{SV}^2(B,D,M,S) + \frac{1}{K_0(B,D,M)} \sum_{S=1}^{SV\_B\_SIZE} \left[U_1(B,D,M,S) - U_2(B,D,M,S) \right] \right\}^{1/2}$
Operational	$S_0(B,D,1) = \sqrt{\frac{1}{\sum_{M=1}^{2} K_0(B,D,M)}} \left\{ \sum_{M=1}^{2} \sum_{S=1}^{SV\_B\_SIZE} (N_{SV}(B,D,M,S) - 1)\ S_{SV}^2(B,D,M,S) + \frac{1}{\sum_{M=1}^{2} K_0(B,D,M)} \sum_{M=1}^{2} \sum_{S=1}^{SV\_B\_SIZE} \left[U_1(B,D,M,S) - U_2(B,D,M,S) \right] \right\}^{1/2}$

where

$$U_1(B,D,M,S) = N_{SV}(B,D,M,S)\ \left(K_0(B,D,M) - N_{SV}(B,D,M,S)\right)\ \overline{DN}_{SV}^2(B,D,M,S)$$

$$U_2(B,D,M,S) = 2 \sum_{T>S}^{SV\_B\_SIZE} N_{SV}(B,D,M,S)\ N_{SV}(B,D,M,T)$$

An incremental form of the quantities above would reduce processor loading as new SV scan statistics are shifted in and out of the SV buffer.

2.8 SV Buffer Order Statistics

In order to implement the outlier test described in Section 2.1 the extreme values of the SV buffer must be updated.

Processing	SV Buffer Order Statistics
Solar calibration	$MN_0^0(B,D,M) = \mathrm{Min}\left[MN_{SV}(B,D,M,S)\right]_{S=1}^{S=SV\_B\_SIZE}$ $MX_0^0(B,D,M) = \mathrm{Max}\left[MN_{SV}(B,D,M,S)\right]_{S=1}^{S=SV\_B\_SIZE}$ $MN_0^1(B,D,M) = \min\left[MN_{SV}(B,D,M,S)\right]_{S=1}^{S=SV\_B\_SIZE}$ $MX_0^1(B,D,M) = \max\left[MN_{SV}(B,D,M,S)\right]_{S=1}^{S=SV\_B\_SIZE}$
Operational	$MN_0^0(B,D,1) = \mathrm{Min}\left[MN_{SV}(B,D,M,S)\right]_{S=1,M=1}^{S=SV\_B\_SIZE,M=2}$ $MX_0^0(B,D,1) = \mathrm{Max}\left[MN_{SV}(B,D,M,S)\right]_{S=1,M=1}^{S=SV\_B\_SIZE,M=2}$ $MN_0^1(B,D,1) = \min\left[MN_{SV}(B,D,M,S)\right]_{S=1,M=1}^{S=SV\_B\_SIZE,M=2}$ $MX_0^1(B,D,1) = \max\left[MN_{SV}(B,D,M,S)\right]_{S=1,M=1}^{S=SV\_B\_SIZE,M=2}$

where if $X = [X_1, X_2, ..., X_m]$, then $\mathrm{Min}(X) = X_{(1)}$, $\min(X) = X_{(2)}$, $\mathrm{Max}(X) = X_{(m)}$, and $\max(X) = X_{(m-1)}$.

3 Process SD Scans

The SD processing section of L1B executes only when the SD has been deployed. Here we assume MODIS is not in A&E, and that L1B algorithm is in operational execution about to process SD count data. The SD is illuminated with the state of the SD screen known (up or down), and that the responsivities of the applicable detectors (as per Table 1) are to be estimated. During the SD illumination period the MODIS mirror will scan the SD for approximately 2 minutes.

Table 3.1
SD Array Indexing

Variable	Description	Range
B	Band. Solar reflective bands: 1-19, 26.	1:20
D	Detector.	$1{:}N_D(B)$[1]
M	Mirror side.	1:2
S	SD scan.	1:SD_B_SIZE
F	SD sample.	1:60 bands 1-2 1:30 bands 3-7 1:15 bands 8-19,26

[1] See Table 1.1

Table 3.2
SD Variable Definition

Variable	Description
$DN_{SD}(B,D,M,F)$	SD scan data. SD scan vector has B, D, and M fixed.
$N_{SD}(B,D,M,S)$	Number of SD samples in one scan (≤ 30, 60, 120)
$\overline{DN}_{SD}(B,D,M,S)$	Average SD count for scan S
$K_{SD}(B, D,M)$	Total number of SD scans (≤ SD_B_SIZE)

Table 3.3
SD Control Parameters

Parameter	Description
SD_B_SIZE	Number of scans in SD buffer
FSD	SD sector starting sample number ($FSD + N_{SD} \le 15, 30, 60$)

3.1 SD Scan Average

The samples from the SD for each scan of the SD object space sector are averaged. Each scan average will subsequently be used as the dependent variables in a linear regression equation that will produce estimates of the detector responsivities. Over the nominal 2 minute collection interval 81 scans will produce averages for all detectors in the solar reflective bands and two mirror sides.

$$\overline{DN}_{SD}(B,D,M,S) = \frac{1}{N_{SD}(B,D,M,S)} \sum_{F=FSD}^{F=FSD+N_{SD}(B,D,M,S)} DN_{SD}(B,D,M,F)$$

3.2 Increment SD Scan Counter

$K_{SD}(B,D,M)$ is incremented for each new scan.

4 Process Geometrical Variables Synchronized with SD Scans

The radiance of the SD depends on the solar incidence angle, the SD Bidirectional Reflectance Distribution Function (BRDF), and the transmittance of the SD attenuation screen (when used). The quantities in this section represent averages over the samples in each scan segment. The subscript "F" indicates that the quantity is to be evaluated at the SD scan sample level. The geometrical quantities calculated here will be needed to determine the relation between detector output and radiance as measured in Section 2. Thus all the quantities in this section must be stored in arrays whose elements have a one-to-one time-correspondence with the average detector count data of Sections 2 and 3.

Two solar angles relative to the SD (θ_{Geo} and φ_{Geo}) are available to L1B in the Geolocation data product at the scan level [MCST, 1995]. The solar direction is available from SDP Toolkit calls and is needed for SDSM incidence angle calculation in Section 5 [EOSDIS]. SD screen transmittance and solar irradiance reside in look-up tables. Table look-up and the corresponding interpolations are denoted by the symbol "LUT[·]". Information accessible from the Geolocation data set appears with the subscript "Geo" in the development below.

Table 4.1
Geometry Array Indexing

Variable	Description	Range
M	Mirror side	1:2
S	SD Scan	1:SD_B_SIZE
F	SD sample	1:64 bands 1-2 1:32 bands 3-7 1:16 bands 8-19,26
t	Time	1: TOTAL_CAL

Table 4.2

Geometry Variable Definition

Variable	Description
$\cos(\theta_{SD})(M,S)$	Cosine of the angle between the solar vector and the SD normal.
$\cos(\theta_{SDSM})(M,S)$	Cosine of the angle between the solar vector and the SDSM screen.
$\varphi_{SD}(M,S)$	Solar azimuth angle relative to the SD x-axis
SD_YEAR (t)	Time array (year + fraction-of-year)
$E_{sun}(B)$	Solar irradiance in the MODIS bands 1-19, and 26
$U_{sun}(3,M,S)$	Solar direction unit vector in ECI coordinates
$U_{SDSM}(3)$	SDSM screen unit vector in MODIS coordinates
$\bar{\tau}_{SD}(M,S)$	SD screen transmittance for the current scan and mirror side
$\overline{BRDF}_{SD}(B,M,S)$	SD BRDF measurements at relevant bidirectional angles

Table 4.3

Geometry Control Parameters

Parameter	Description
TOTAL_CAL	Total number of SD calibration periods in the mission

Table 4.4

Geometry Data Tables

Table	Description
SOLAR_IRRAD	Solar irradiance band-integrated for MODIS bands 1-19, 26
SD_SCREEN_T	SD screen transmittance
SD_BRDF	Prelaunch SD BRDF
SDSM_SCREEN	Unit vector containing the SDSM screen normal

4.1 Cosine of the Angle Between the Solar Vector and the SD Normal

The SD radiance is a function of the solar incidence angle, changing approximately 20-25% during the solar calibration period. The solar incidence angle is not a function of band nor detector and is available in the Geolocation data product at the scan level [MCST, 1995].

$$\cos(\theta_{SD})(M,S) = \cos(\theta_{Geo}(M,S))$$

4.2 Solar Azimuth Angle on SD

The solar azimuth angle is neither a function of band nor detector and is available in the Geolocation data product at the scan level [MCST, 1995].

$$\varphi_{SD}(M,S) = \varphi_{Geo}(M,S)$$

4.3 Cosine of the Angle Between the Solar Vector and the SDSM Screen

The solar direction is available as unit vector from SDP Toolkit calls, and the SDSM screen normal resides in a data table expressed as a unit vector in the ECI reference frame. Let U_{sun}, and U_{SDSM} denote each of these quantities, respectively. Since the SDSM count data (see Section 5) will need to be synchronized with the SD data, compute the SDSM solar incidence angle for each scan time of the SD as

$$\cos(\theta_{SDSM})(M,S) = \sum_{i=1}^{3} U_{sun}(i, M,S)\ \ U_{SDSM}(i)$$

4.4 Time of SD Calibration Period

The year and fraction-of-year should be computed for the mid-point of the SD calibration period and stored in the SD time vector. Time information is available from the L1A data product.

$$SD\_YEAR\,(t) = year_{L1A} + day_{L1A} / 365.25$$

4.4 Sun-Earth Distance Correction to Solar Irradiance

The ratio of the square of the mean Sun-Earth distance (1 AU) to the current Sun-Earth distance is sufficiently accurate when computed as

$$\begin{aligned} R_T = {} & 1.000110 + 0.034221\ \cos\ (2\pi T) + 0.001280\ \sin\ (2\pi T) + \\ & 0.000719\ \cos\ (4\pi T) + 0.000077\ \sin\ (4\pi T) \end{aligned}$$

where T is the fraction of the year ($day_{L1A} / 365.25$) [Paltridge and Platt, 1976].

4.5 Solar Irradiance at 1 AU

The solar spectral irradiance at 1 AU is estimated using the MODIS prelaunch radiance calibration as monitored by the SRCA during A&E, or from optional sources. Its value is stored in the table SOLAR_IRRAD, and will periodically be updated based on Science Team recommendations. Updates could be adjustments to compensate for spectral band-shifts occurring in the MODIS filters as the filters degrade throughout the mission, or adjustments derived from detector responsivity changes. The solar spectral irradiance is denoted as $E_{sun}(B)$. The distance correction, R_T, is multiplied with the solar irradiance in order to compensate for the varying sun-earth distance. The solar irradiance at year-fraction time T is given by $R_T E_{sun}(B)$.

4.6 SD Screen Transmittance

The SD screen transmittance is a function of screen design parameters and solar incidence angles, and is designed around the nominal value of 0.085. Screen transmittance resides in the table SD_SCREEN_T. A bilinear interpolation is needed to get the transmittance for the current scan's solar angles.

$$\bar{\tau}_{SD}(M,S) = LUT[SD\_SCREEN\_T, \theta_{SD}(M,S), \varphi_{SD}(M,S)]$$

4.7 SD BRDF

The SD BRDF is measured pre-launch, for a range of bidirectional angles specific to MODIS. The measurements reside in the table SD_BRDF, which is a function of MODIS band, and local SD coordinates of the sun vector (θ,φ) as determined in Sections 4.1 and 4.2.

$$\overline{BRDF}_{SD}(B,M,S) = LUT[SD\_BRDF(B), \theta_{SD}(M,S), \varphi_{SD}(M,S)]$$

5 Process SDSM Measurements

The SDSM operates independently from the other MODIS OBCs, and collects three samples every 1.5 s during the solar calibration period. The three values are averaged to produce one sample per 1.5 s, and the digital count values (CN) referenced below will denote the average over this time interval. The SDSM collects three samples sequentially at each of four positions.

SDSM Cycle

Position	Count	Source	Description
1	CN_{sun}	Sun	solar flux enters SDSM cavity through screen
2	CN_0	Dark	no solar flux enters SDSM cavity
3	CN_{SD}	SD	solar flux reflects from SD and enters SDSM cavity
4	CN_0	Dark	no solar flux enters SDSM cavity

Since the sampling time is 1.5 s, the SDSM cycle takes 6 s to complete. This cycle is repeated throughout the nominal 2 minute SD illumination period, and thus 20 sample averages are available for each of the SDSM positions.

The SDSM has 9 detectors with spectral filters similar to a subset of the MODIS solar reflective bands. In order to utilize the SDSM measurements in 9 bands to estimate the SD degradation in the solar reflective bands of MODIS, an interpolation/extrapolation scheme must be employed. Extrapolation is needed for MODIS bands 5-7, and 26. Linear interpolation using the two bounding neighbors is adequate for interpolation. Extrapolation to the MODIS bands whose wavelengths are larger than SDSM band 9 is performed by using the SD degradation at SDSM band 9,

The SDSM views the sun through an aperture containing a filter with a nominal 2% transmission. The solar incidence angle onto the screen must be known to account for the projection of the SDSM aperture onto the incoming solar flux. As the SDSM samples SD radiance the SD solar geometry is needed at the SDSM sample times. All four SDSM measurements made during a 6 s SDSM cycle must be synchronized with the SD measurements being made by the MODIS detectors.

Table 5.1
SDSM Array Indexing

Variable	**Description**	**Range**
B	SDSM band.	1:9
B_{SD}	SD band.	1:20
S	SDSM scan.	1:SDSM_B_SIZE
S_{SD}	SD scan.	1:SD_B_SIZE
t	Time.	1: TOTAL_CAL

Table 5.2
SDSM Variable Definition

Variable	Description
$\cos(\theta_{SD})(M,S_{SD})$	Cosine of the angle between the solar vector and the SD normal.
$\cos(\theta_{SDSM})(M,S_{SD})$	Cosine of the solar vector relative to the SDSM screen normal.
$\varphi_{SD}(M,S_{SD})$	Solar azimuth angle relative to the SD x-axis from Section 4.6.
$\bar{\tau}_{SD}(M,S_{SD})$	SD screen transmittance from Section 4.6.
$\overline{CN}_{SD}(B,S)$	Average of 3 SDSM count values from one SD sample.
$\overline{CN}_{sun}(B,S)$	Average of 3 SDSM count values from one Sun sample.
$\overline{CN}_{0}(B,S)$	Average of 6 SDSM count values from two dark samples.
$N_{SDSM}(B)$	Number of SDSM scans during solar cal. period (≤SDSM_B_SIZE).
BRDF(B,S)	SD BRDF factor derived from 9 bands of SDSM data.
$BRDF_{A\&E}(B,S)$	SD BRDF factor derived from 9 bands of SDSM data in A&E
$\cos(\theta_{SD\_SUN})(S)$	$\cos(\theta_{SD})(M,S_{SD})$ interpolated to SDSM samples.
$\cos(\theta_{SDSM\_SUN})(S)$	$\cos(\theta_{SDSM})(M,S_{SD})$ interpolated to SDSM samples.
$\varphi_{SD\_SUN}(S)$	$\varphi_{SD}(M,S_{SD})$ interpolated to SDSM samples.
$\tau_{SD}(S)$	SD screen transmittance interpolated from $\bar{\tau}_{SD}(M,S_{SD})$.
τ_{SDSM}	SDSM screen transmittance (nominal 2%).
$\Delta_{SDSM}(B,t)$	SD degradation estimates at the 9 SDSM bands.
$\Delta(B_{SD}, t)$	SD degradation estimates at the solar reflective MODIS bands.

Table 5.3
SDSM Control Parameters

Parameter	Description
SDSM_B_SIZE	Number of SDSM scan cycles in solar calibration period
TOTAL_CAL	Total number of SD calibration periods in the mission
MAX_REJECT	Maximum number of outliers rejected in one sample

Table 5.4
SDSM Data Tables

Table	Description
SOLAR_IRRAD	Solar irradiance band-integrated for MODIS bands 1-19, 26
SD_SCREEN_T	SD screen transmittance
SD_BRDF	Prelaunch SD BRDF
BRDF_A&E	SDSM BRDF factor computed during A&E.

5.1 Filter SDSM Count Values

Using the outlier algorithm described in Section 2, filter raw SDSM samples (3 samples per 1.5 s) using the combined data from each SDSM band for all the cycles in three separate steps: (1) solar samples, (2) SD samples, and (3) dark samples. The order statistics used during each band's check are those computed from each scan's sample. Decrement $N_{SDSM}(B)$ if outliers are found, and do not reject more than MAX_REJECT samples per combined sample.

5.2 Interpolate Geometrical Data to SDSM Cycle Times.

Table 5.2 shows that the solar angles and transmittances are indexed with the SD scan counter S_{SD} and mirror side M since these quantities are being carried from the SD processing section into the SDSM section. The SDSM scan index S is different than S_{SD} since the SD and SDSM sampling rates differ. In order to utilize the angular and transmittance information in this section, it is necessary to interpolate from the (M, S_{SD}) index space of the SD to the scan index space (S) of the SDSM. This is accomplished by using the system time vector for synchronization between the two spaces. The resulting interpolated arrays are $\cos(\theta_{SD\_SUN})(S)$, $\cos(\theta_{SDSM\_SUN})(S)$, $\varphi_{SD\_SUN}(S)$, and $\tau_{SD}(S)$.

5.3 Estimate SD BRDF from the View Angle of the SDSM

The bidirectional angles at which the SDSM samples the SD radiance are the zenith and azimuth angles θ_{SD_SDSM}, and φ_{SD_SDSM}. These angles differ from their counterparts in the MODIS scan mirror sampling of the SD radiance. Thus the SD BRDF estimate to be derived from the SDSM sampling technically represents the SD/SDSM bidirectional configuration. The working assumption in the L1B algorithm is that any SD degradation that may occur through time at the SD/SDSM configuration is identical to the degradation which would occur in the SD/MODIS bidirectional configuration. At each SDSM cycle point, the estimate of the SD BRDF is, up to a scaling constant

$$\mathrm{BRDF}\,(B,S) = \frac{(\,\overline{CN}_{SD}(B,S) - \overline{CN}_{0}(B,S)\,)\quad \tau_{SDSM}\ \ \cos(\theta_{SDSM\_SUN})(S)}{(\,\overline{CN}_{SUN}(B,S) - \overline{CN}_{0}(B,S)\,)\quad \tau_{SD}(S)\ \ \cos(\theta_{SD\_SUN})(S)}$$

5.4 Interpolate $BRDF_{A\&E}$ to the Viewing Geometry of BRDF

The procedure in Section 5.3 is utilized during A&E to obtain the BRDF factor which characterizes the SD before degradation has occurred. The ratio between the BRDF factors obtained in Section 5.3 and that obtained during A&E is a measure of the degradation of the SD BRDF. In order that this ratio accurately represent the degradation, the effects of different viewing configurations between A&E and the current time must be taken into account. This is done by using the look-up table BRDF_A&E to perform a bilinear interpolation of the BRDF measured in A&E to the bidirectional angles implicit in the BRDF factor computed in Section 5.3. The angular variables in the table BRDF_A&E are θ_{SD} and φ_{SD}.

$$BRDF_{A\&E}(B,S) = LUT[\ BRDF\_A\&E, \theta_{SD}(S), \varphi_{SD}(S)\ ]$$

5.5 Estimate SD BRDF Degradation at the View Angle of the SDSM

The SD degradation at the SDSM wavelengths is estimated from the average of the ratios of the SDSM BRDF estimates at time t, subsequent to A&E, to that at A&E as

$$\Delta_{SDSM}(B,t) = \frac{1}{N_{SDSM}(B)} \sum_{S=1}^{N_{SDSM}(B)} \frac{BRDF(B,S)}{BRDF_{A\&E}(B,S)}$$

5.6 Interpolate/Extrapolate SD BRDF Degradation to the MODIS Bands

Linear interpolation is used to get estimates of the SD degradation (Δ) at the MODIS wavelengths. Bands 5-7, and 26 have wavelengths longer than those of the SDSM. Since Δ is not expected to be large at these longer wavelengths, the degradation estimated at MODIS band 19 should be used at bands 5-7, and 26. Table 1.3 contains the SDSM band numbers and wavelengths. The SD degradation is derived from $\Delta_{SDSM}(B,t)$ and is denoted as

$$\Delta(B_{SD}, t)$$

6 Detector Responsivity Estimation

After the SD scans have been processed, the SD radiance can be estimated. The detectors of the MODIS solar reflective bands respond linearly to irradiance when not saturated, hence the detector responsivity is the proportionality constant linking detector digitized counts with SD radiance. As the SD progresses through a solar encounter, its radiance will change in response to the changing solar incidence geometry. It can also be assumed that the offset-corrected detector output when the SD is not illuminated will be zero on average. These assumptions indicate that a zero-intercept straight-line regression model could be used to regress offset-corrected detector counts on calculated SD radiance to estimate detector responsivity [Seber, 1977].

Table 6.1
Array Indexing

Variable	Description	Range
B	Band	1:20
D	Detector	1:N_D(B)
S	SD scan	1:SD_B_SIZE
t	Time	1: TOTAL_CAL

Table 6.2
Variables for Responsivity Estimation

Variable	Description	Sec.
R_T	Solar irradiance adjustment factor for sun-earth distance.	4.4
$E_{sun}(B)$	Solar irradiance in the MODIS bands 1-19, and 26.	4.5
$\bar{\tau}_{SD}(M,S)$	SD screen transmittance.	4.6
$\Delta(B,t)$	SD degradation at the MODIS solar reflective bands.	5.6
$\overline{BRDF}_{SD}(B,M,S)$	Prelaunch SD BRDF measurements.	4.6
$\cos(\theta_{SD})(M,S)$	Cosine of the solar vector relative to the SD normal.	4.1
$\overline{DN}_{SD}(B,D,M,S)$	Average SD effective count for scan S.	3.1
$K_{SD}(B, D,M)$	Total number of SD scans (≤ SD_B_SIZE).	3.2
$L_{SD}(B,M,S)$	SD Radiance.	6.1
$DN_{SD}(B,D,M,S)$	Effective SD detector count for scan S.	6.2
$_L(B,D, M)$	Radiance responsivity.	6.4
$S_L(B,D)$	Standard error of the radiance responsivity.	6.6
$_\rho(B,D)$	Reflectance calibration coefficient.	6.7
$S_\rho(B,D)$	Standard error of the reflectance responsivity.	6.7
R(B, M)	Relative reflectance of the scan mirror sides.	6.5
SD_YEAR(t)	Time array.	4.4
$N_t(B,D)$	Current number of SD calibration periods (≤ TOTAL_CAL)	6.8

Table 6.3
Responsivity Control Parameters

Parameter	Description
SD_B_SIZE	Total number of SD scans
TOTAL_CAL	Total number of SD calibration periods in the mission

Table 6.4

Mirror Reflectivity Data Table

Table	Description
MIRROR_REFL	Relative reflectivity of scan mirror sides
RESP_RECORD	Table containing responsivity records and SD_YEAR(t)

6.1 SD Radiance

The SD radiance during a solar encounter is given by the quantities computed in Sections 2-5 as

$$L_{SD} = R_T \ E_{sun} \ \bar{\tau}_{SD} \ \ \Delta \overline{BRDF}_{SD} \ \cos(\theta_{SD})$$

where array indexing has been omitted for clarity. This relation holds for a given MODIS band at a specific time). Using the notation of Tables 3.1 and 4.1 the array form of this equation becomes

$$L_{SD}(B,M,S) = R_T \ E_{sun}(B) \ \bar{\tau}_{SD}(M,S) \ \ \Delta(B,t) \ \overline{BRDF}_{SD}(B,M,S) \ \cos(\theta_{SD})(M,S)$$

The radiance depends on the band (B) since it is wavelength dependent. It is not dependent on detector since all detectors within a band share the same filter. Synchronization is maintained with the M and S indexes.

6.2 Filter SD Counts

The linear relationship between offset-corrected SD counts and SD radiance can be utilized to reduce the variability of either $L_{SD}(B,D,M,S)$ or $DN_{SD}(B,D,M,S)$ by computing their ratio over all elements in a scan (S) for a given band (B), detector (D), and mirror side (S). Using the outlier algorithm described in Section 2, filter this ratio over the scan variable. The order statistics used during each check are computed from the scan's sample. Decrement $N_{SD}(B,D,M)$ if outliers are found, and do not reject more than MAX_REJECT samples per scan. Using the nomenclature of Section 2.1 a sample call is

$$\text{DN\_FILTER}(\ DN_{SD}(B,D,M,*)/\ L_{SD}(B,D,M,*),,,,N_{SD}(B,D,M)\ )$$

where the '*' denotes the filtering process is performed on all data residing in the corresponding dimension, and the four missing arguments represent the sample order statistics.

6.3 Radiance Responsivity Estimation for Each Mirror Side

The linear regression model relating effective SD counts to SD radiance for a given detector , band, and mirror side has the matrix form

$$\mathbf{DN}_{SD}(B, D, M) = {}_{L}\mathbf{L}_{SD}(B, M) + \varepsilon$$

where ${}_{L}$ is the detector responsivity for a given band, and mirror side; and ε is a measure of the statistical error of the overall fit of the data to the model, and is a vector of independent gaussian random variables with zero mean and variance σ^2. The data for obtaining an estimate of the responsivity are the measured offset-corrected detector counts and radiances for each scan. Expressing the equation above in component form we have

$$\begin{bmatrix} \overline{DN}_{SD}(B,D,M,1) \\ \overline{DN}_{SD}(B,D,M,2) \\ \\ \\ \\ \\ \overline{DN}_{SD}(B,D,M,K_{SD}(B,D,M)) \end{bmatrix} = \begin{bmatrix} L_{SD}(B,M,1) \\ L_{SD}(B,M,2) \\ \\ \\ \\ \\ L_{SD}(B,M,K_{SD}(B,D,M)) \end{bmatrix} \left[{}_{L} \right] + \begin{bmatrix} \varepsilon_{B,D,M,1} \\ \varepsilon_{B,D,M,2} \\ \\ \\ \\ \\ \varepsilon_{B,D,M,K_{SD}(B,D,M)} \end{bmatrix}$$

The least-squares estimate of the responsivity for a given detector, band, and mirror side is

$${}_{L}(B, D, M) = \frac{\mathbf{L}_{SD}^{T}(B,M)\,\mathbf{DN}_{SD}(B,D,M)}{\mathbf{L}_{SD}^{T}(B,M)\,\mathbf{L}_{SD}(B,M)}$$

where T denotes transpose, ${}_{L}(B,D,M)$ is the array containing the responsivity estimate for each detector within a band for each mirror side. The radiances and offset-corrected count values are written as bold-faced to indicate they are vectors formed from all elements along the scan index (S).

6.4 Mirror Side Correction Factor

Jones [1995] describes the method for obtaining the factor for adjusting the raw detector count values as a pre-processing step before entry into the solar reflective band calibration algorithm. One of these steps is the multiplication of each detector count by a factor to account for any relative reflectivity changes between both scan mirror sides which may occur through mission life. This relative reflectivity is estimated in this section from the responsivities computed in the previous section, and is dependent only on band and mirror side. The relative reflectivity estimates are updates to the current values and are given by

$$R(B,M) = \frac{\dfrac{2\sum_{D=1}^{N_D(B)} {}_{L}(B,D,M)}{R(B,M)}}{\dfrac{\sum_{D=1}^{N_D(B)} {}_{L}(B,D,1)}{R(B,1)} + \dfrac{\sum_{D=1}^{N_D(B)} {}_{L}(B,D,2)}{R(B,2)}}$$

After computation, R(B,M) should be appended to the mirror reflectivity data table MIRROR_REFL for future reference.

6.5 Combine SV Buffer Statistics

For all subsequent processing the mirror side segregation is not necessary. In order for the SV buffer statistics to be representative of SV data from both sides of the scan mirror the data in the SV buffer arrays for M=1 and 2 must be combined and placed into the M=1 location. Subsequent references to the array $_{L}$ will omit the "M" index.

6.6 Radiance Responsivity Estimation

The linear regression model relating average effective counts to SD radiance for a given detector , band, and mirror side has a form identical to the form in Section 6.3, except that now the mirror sides are not differentiated.

$$\mathbf{DN}_{SD}(B,D) = {}_{L}\mathbf{L}_{SD}(B) + \varepsilon$$

where $_{L}$ is the detector responsivity for a given band, and ε is the measure of the residual variance, σ^2, of the overall fit of the data to the. The input data are the measured offset-corrected detector counts and radiances for each scan, and mirror side. Expressing the equation above in component form we have

$$\begin{bmatrix} \overline{DN}_{SD}(B,D,1,1) \\ \overline{DN}_{SD}(B,D,2,1) \\ \\ \\ \\ \\ \overline{DN}_{SD}(B,D,2,K_{SD}(B,D,2)) \end{bmatrix} = \begin{bmatrix} L_{SD}(B,1,1) \\ L_{SD}(B,2,1) \\ \\ \\ \\ \\ L_{SD}(B,2,K_{SD}(B,D,2)) \end{bmatrix} \left[\ {}_{L}\ \right] + \begin{bmatrix} \varepsilon_{B,D,1,1} \\ \varepsilon_{B,D,2,1} \\ \\ \\ \\ \\ \varepsilon_{B,D,2,K_{SD}(B,D,2)} \end{bmatrix}$$

Each column vector now contains $K_{SD}(B,D,1)+ K_{SD}(B,D,2)$ elements. The least-squares estimate of the responsivities $^{B,D}_{L}$ for a given detector, and band is

$${}_{L}(B,D) = \frac{\mathbf{L}^{T}_{SD}(B)\,\mathbf{DN}_{SD}(B,D)}{\mathbf{L}^{T}_{SD}(B)\,\mathbf{L}_{SD}(B)}$$

where T denotes transpose, and ${}_{L}(B,D)$ is the array containing the responsivity for each detector within a band. The radiances and offset-corrected count values are written as bold-faced to indicate they are vectors formed from all elements along the mirror index (M), and scan index (S). The estimate of σ^2 is

$$S^2(B,D) = \frac{\left(\mathbf{DN}_{SD}(B,D) - {}_{L}(B,D)\ \mathbf{L}_{SD}(B)\right)^T \left(\mathbf{DN}_{SD}(B,D) - {}_{L}(B,D)\ \mathbf{L}_{SD}(B)\right)}{K_{SD}(B,D,1) + K_{SD}(B,D,2) - 1}$$

and the standard error of the radiance responsivity is given by

$$S_L(B,D) = S(B,D)\ \sqrt{\mathbf{L}^T_{SD}(B)\ \mathbf{L}_{SD}(B)}$$

6.7 Reflectance Calibration Coefficient

In order to calibrate the detectors with respect to EV BRF the radiance responsivities, ${}_{L}$, for each band and detector as calculated above are utilized. The BRF calibration coefficient is given by

$${}_{\rho}(B,D) = \frac{R_t\ \ E_{sun}(B)\ \ {}_{L}(B,D)}{\pi}$$

where t is the fraction of the year for the current scan. The BRF calibration coefficient is time dependent.

The standard error of the reflectance calibration coefficient is given by

$$S_{\rho}(B,D) = \frac{R_t\ \ E_{sun}(B)\ \ S_L(B,D)}{\pi}$$

6.8 Responsivity Record File

The radiance responsivity, ${}_{L}$, and standard error, S_L, as estimated in Section 6.6, will serve as the basis for a responsivity prediction function. Hence these parameter estimates and their associated variances must be appended to the table RESP_RECORD that will subsequently be referenced after each SD calibration period. The radiance responsivities must be time-tagged with the vector SD_YEAR, and the SD calibration period counter, $N_t(B,D)$ incremented by one.

7 Responsivity Prediction and Trending

Data from heritage instruments indicate that for a given irradiance detector output can change throughout mission life, either increasing or decreasing over long time scales relative to the sampling frequency of the detector. The causes may be due to optical component degradation such as lens coating deterioration, filter bandpass changes, contamination, or other effects. In order to model a detector's degradation, a piecewise linear function of time is used to predict the detector's responsivity. The parameters of this linear function are estimated using the responsivity record generated from the SD calibration periods.

The treatment in the following sections considers radiance responsivity only. The BRF calibration coefficient trending is a function of the radiance responsivity as shown in Section 6.7.

Note the redefinition of the responsivity and standard error arrays which now include a new dimension indexed by "t" which allows the entire responsivity record to fit into a single array. It is left to the implementor to recast the affected arrays or use alternatives.

Table 7.1
Array Indexing

Variable	Description	Range
B	Band.	1:20
D	Detector.	$1{:}N_D(B)$
t	Time .	1: TOTAL_CAL

Table 7.2

Variables for Responsivity Prediction

Variable	Description	Sec.
$_{L}(B,D,t)$	Radiance responsivity for band B, detector D, at time t.	6.6
SD_YEAR(t)	Time of SD calibration periods.	4.4
$N_t(B,D)$	Number of SD calibration periods (≤ TOTAL_CAL).	6.8
$S_L(B,D,t)$	Standard error of the radiance responsivity.	6.6
$b_0(B, D)$	Intercept of responsivity prediction.	7.1
$b_1(B, D)$	Slope of responsivity prediction.	7.1
$\overline{\ }_{L}(B,D)_w$	Weighted mean radiance responsivity.	7.1
$\overline{SD\_YEAR}_w$	Weighted mean year.	7.1
Y	Time (year + day / 365.25).	
$S_{wL}(B,D)$	Residual std. dev. of radiance responsivity prediction.	7.1
$^{*}_{L}(B,D)_Y$	Radiance responsivity prediction.	7.2
$S^{*}_{L}(B,D)_Y$	Radiance responsivity prediction std. dev.	7.3
$^{*}_{\rho}(B,D)_Y$	Reflectance calibration coefficient prediction.	
$S^{*}_{\rho}(B,D)_Y$	Reflectance calibration coefficient prediction std. dev.	

Table 7.3

Responsivity Prediction Control Parameters

Parameter	Description
TOTAL_CAL	Total number of SD calibration periods in mission
RESP_REJECT_LEVEL	Responsivity outlier test level for F_TABLE (sec. 7.5)

Table 7.4

Responsivity Prediction Data Tables

Table	Description
RESP_RECORD	File containing responsivity records and SD_YEAR(t)
F_TABLE	Percentage points of the F distribution (sec. 7.5)

7.1 Radiance Responsivity Prediction Model

The linear model for responsivity has the form

$$= \beta_0 + \beta_1 t + \varepsilon$$

where   is the responsivity; β_0 and β_1 parameters to be estimated for each band and detector; t is time, and ε the error term. In component form the problem becomes

$$\begin{bmatrix} {}_L(B,D,1) \\ {}_L(B,D,2) \\ \\ \\ \\ \\ {}_L(B,D,N_t(B,D)) \end{bmatrix} = \begin{bmatrix} 1 & SD\_YEAR(1) \\ 1 & SD\_YEAR(2) \\ & \\ & \\ & \\ & \\ 1 & SD\_YEAR(N_t(B,D)) \end{bmatrix} \begin{bmatrix} \beta_0 \\ \beta_1 \end{bmatrix} + \begin{bmatrix} \varepsilon(B,D)_1 \\ \varepsilon(B,D)_2 \\ \\ \\ \\ \\ \varepsilon(B,D)_{N_t(B,D)} \end{bmatrix}$$

where the responsivity and time are read from the responsivity-trend record RESP_RECORD. The variances of the responsivities calculated in Section 6.7, also read from the responsivity-trend record, will act as weights. Thus the covariance matrix of ε is

$$\sigma^2 \operatorname{diag}\left[S_L^{-2}(B,D,1), S_L^{-2}(B,D,2), \ldots, S_L^{-2}(B,D,N_t(B,D))\right]$$

Define the weighted means

$$\bar{}_L(B,D)_w = \frac{\sum_{t=1}^{N_t(B,D)} \frac{{}_L(B,D,t)}{S_L^2(B,D,t)}}{\sum_{t=1}^{N_t(B,D)} \frac{1}{S_L^2(B,D,t)}}, \quad \overline{SD\_YEAR}_w = \frac{\sum_{t=1}^{N_t(B,D)} \frac{SD\_YEAR(t)}{S_L^2(B,D,t)}}{\sum_{t=1}^{N_t(B,D)} \frac{1}{S_L^2(B,D,t)}}$$

Let b_{0L} and b_{1L} denote the estimates of β_0 and β_1, respectively. Then

$$b_0(B,D) = \bar{}_L(B,D)_w - b_{1L}(B,D)\ \overline{SD\_YEAR}_w$$

$$b_1(B,D) = \frac{\sum_{t=1}^{N_t(B,D)} \frac{\left({}_L(B,D,t) - \bar{}_L(B,D)_w\right)\left(SD\_YEAR(t) - \overline{SD\_YEAR}_w\right)}{S_L^2(B,D,t)}}{\sum_{t=1}^{N_t(B,D)} \frac{\left(SD\_YEAR(t) - \overline{SD\_YEAR}\right)^2}{S_L^2(B,D,t)}}$$

The estimate of σ^2 is given by

$$S_{wL}^2(B,D) = \frac{1}{N_t(B,D)-2}\left\{\sum_{t=1}^{N_t(B,D)} \frac{\left({}_L(B,D,t) - \bar{}_L(B,D)_w\right)^2}{S_L^2(B,D,t)} - b_{1L}^2(B,D) \sum_{t=1}^{N_t(B,D)} \frac{\left(SD\_YEAR(t) - \overline{SD\_YEAR}_w\right)^2}{S_L^2(B,D,t)}\right\}$$

7.2 Radiance Responsivity Prediction

The estimated parameters b_0 and b_1 are used to predict the radiance responsivity from the linear equation

$$^*_L(B,D)_Y = b_0(B,D) + b_1(B,D)\ Y$$

where Y is the time expressed in the units in the vector SD_YEAR.

$^{*}_{L}(B,D)_Y$ is used for all time intervals subsequent to the solar calibration until the next calibration period occurs at which point b_0 and b_1 are re-estimated based on the augmented SD radiance record.

The temporal extent to which the responsivity-trend history is linear will be assessed in the TLCF. Two-phase linear regression [Seber, 1977] techniques will be implemented to determine whether the responsivity-trend history slope has changed. If it is determined that the slope has changed, only the appropriate subset of the data in RESP_RECORD will be used for prediction function parameter estimation.

7.3 Radiance Responsivity Prediction Variance

The variance of $^{*}_{L}(B,D)_Y$ is needed to compute the uncertainty of the L1B radiance product. It is a continuous function of time (Y), and is given by

$$S_L^{*2}(B,D)_Y = S_{wL}^2(B,D)\left\{1 + \frac{1}{\sum\limits_{t=1}^{N_t(B,D)} \frac{1}{S_L^2(B,D,t)}} + \frac{(Y - \overline{\text{SD\_YEAR}}_w)^2}{\sum\limits_{t=1}^{N_t(B,D)} \frac{(\text{SD\_YEAR}(t) - \overline{\text{SD\_YEAR}}_w)^2}{S_L^2(B,D,t)}}\right\}$$

In order for the operational algorithm to produce radiance responsivity uncertainties continuously, the following three quantities will be useful:

$$W_{0L}(B,D) = S_{wL}^2 + \frac{S_{wL}^2}{\sum\limits_{t=1}^{N_t(B,D)} \frac{1}{S_L^2(B,D,t)}}$$

$$W_{1L}(B,D) = \frac{S_{wL}^2}{\sum\limits_{t=1}^{N_t(B,D)} \frac{(\text{SD\_YEAR}(t) - \overline{\text{SD\_YEAR}}_w)^2}{S_L^2(B,D,t)}}$$

and $\overline{\text{SD\_YEAR}}_w$. The radiance responsivity prediction variance then becomes

$$S_L^{*2}(B,D)_Y = W_{0L}(B,D) + W_{1L}(B,D)\ (Y - \overline{\text{SD\_YEAR}}_w)^2$$

7.4 Reflectance Calibration Coefficient Prediction

As in Section 6.7, the BRF calibration coefficient is computed from the radiance responsivity. The predicted value is

$$^{*}_{\rho}(B,D)_Y = \frac{R_{t(Y)}\quad E_{sun}(B)\quad ^{*}_{L}(B,D)}{\pi}$$

where t(Y) is the fraction of the year corresponding to year Y.

7.5 Prediction Interval for Radiance Responsivity

Standard linear regression techniques are used to compute confidence intervals for future radiance responsivity [Seber, 1977]. A 100(1-α)% confidence interval for the radiance responsivity prediction function is the region between the two curves

$$\bar{\ }_{L}(B,D)_w + b_1(B,D)\ \ (Y - \overline{SD\_YEAR}_{\,w}) \pm (2F^{\alpha}_{2,N_t(B,D)-2})^{1/2}\ \ S^{*2}_{L}(B,D)_Y$$

where $F^{\alpha}_{2,N_t(B,D)-2}$ is the 100(1-α) percentage point of the F distribution with 2 and N_t(B,D)-2 degrees of freedom, and $S^{*2}_{L}(B,D)_Y$ is the radiance responsivity prediction variance at year Y computed in Section 7.3.

7.6 Test Current Responsivity Estimates for Inclusion in Prediction Interval

To guard against potential outliers in the process of estimating detector responsivities from SD measurements, the prediction band computed in Section 7.5 will be used to determine whether the radiance responsivity estimates computed in Section 6.6 using the most current solar calibration period are ‘reasonable’. Responsivity estimates falling outside the confidence band of Section 7.5 will not be used in responsivity prediction estimation as described in the previous two sections, and should be flagged for TLCF future processing. The confidence level used in the test scheme is recommended to be 99% corresponding to α=0.01. Rejected responsivities must be flagged in the responsivity record table RESP_RECORD, and not used in responsivity prediction function parameter estimation.

8. Earth View Spectral Radiance and BRF

Once the detector responsivities have been estimated, and the parameters of the responsivity prediction specified the Earth View (EV) radiance and BRF estimation process begins. Along with the SV scan processing component described in Section 2, this section forms the other component of the operational part of the algorithm in the sense that the application of the detector responsivities and offset-correction to detector counts to produce top-of-the-atmosphere EV radiance and BRF occurs here on a scan by scan basis. The SD/SDSM processing described in Sections 3-7 occurs infrequently.

Table 8.1

Array Indexing

Variable	Description	Range
B	Band.	1:20
D	Detector.	$1{:}N_D(B)$
S	Current scan.	1:SV_B_SIZE
t	Time.	1:TOTAL_CAL

Table 8.2

Variables for Earth View Radiances and Reflectances

Variable	Description	Sec.
$DN_{EV}(B,D)$	EV effective count for band B, and detector D.	8.1
$S_{SV}(B,D,1,S)$	SV scan std. dev. for the current scan, band B, det. D.	2.3
$S_0(B,D,1)$	SV buffer std. dev. for band B, and detector D.	2.7
$L_{EV}(B,D)$	EV radiance for band B, detector D.	8.1
$\left[\rho_{EV}\cos(\theta_{EV})\right](B,D)$	EV BRF-(cosine zenith angle) product.	8.1
Y	Time (year + day / 365.25).	
${}^{*}_{L}(B,D)_Y$	Radiance responsivity prediction.	7.2
${}^{*}_{\rho}(B,D)_Y$	Reflectance calibration coefficient prediction.	7.4
$S^{*}_{L}(B,D)_Y$	Radiance responsivity prediction standard error.	7.2
$S_{EV,L}(B,D)$	Standard error of EV radiance, band B, detector D.	8.2
$S_{EV,\rho}(B,D)$	Standard error of EV BRF, band B, detector D.	8.2
$S^{sys}_{L}(B,D)$	Systematic uncertainty in radiance calibration (1σ).	9.8
$S^{sys}_{\rho}(B,D)$	Systematic uncertainty in reflectance calibration (1σ).	9.8
$F_{VC,L}(B)$	Vicarious calibration correction for radiance	9.8
$F_{VC,\rho}(B)$	Vicarious calibration correction for reflectance	9.8

Table 8.3

Responsivity Prediction Data Tables

Table	Description
VC_RADIANCE	Vicarious calibration coefficient correction for radiance by band.
VC_BRF	Vicarious calibration coefficient correction for reflectance by band.
SYS_RADIANCE	MODIS systematic uncertainties for radiance by band and detector.
SYS_BRF	MODIS systematic uncertainties for reflectance by band and detector.

8.1 EV Radiance and BRF Estimates

The Earth View radiance from MODIS effective detector counts is

$$L_{EV}(B,D) = \frac{DN_{EV}(B,D)}{F_{VC,L}(B)\ \ {}^{*}_{L}(B,D)_{Y}}$$

The product of EV BRF with cosine of solar incidence from MODIS effective detector counts is

$$\left[\rho_{EV}\cos(\theta_{EV})\right](B,D) = \frac{DN_{EV}(B,D)}{F_{VC,\rho}(B)\ \ {}^{*}_{\rho}(B,D)_{Y}}$$

8.2 EV Radiance and BRF Uncertainties

The standard errors for the EV radiance and reflectance are based on a first-order approximation.

$$S_{EV,L}(B,D)_{Y} = L_{EV}(B,D)\sqrt{\frac{S^{2}_{SV}(B,D,1,S)+S^{2}_{0}(B,D,1)}{DN^{2}_{EV}(B,D)} + \left(\frac{S^{*}_{L}(B,D)_{Y}}{{}^{*}_{L}(B,D)_{Y}}\right)^{2} + \left(S^{sys}_{L}(B,D)\right)^{2}}$$

$$S_{EV,\rho}(B,D)_{Y} = \left[\rho_{EV}\cos(\theta_{EV})\right](B,D)\sqrt{\frac{S^{2}_{SV}(B,D,1,S)+S^{2}_{0}(B,D,1)}{DN^{2}_{EV}(B,D)} + \left(\frac{S^{*}_{L}(B,D)_{Y}}{{}^{*}_{L}(B,D)_{Y}}\right)^{2} + \left(S^{sys}_{\rho}(B,D)\right)^{2}}$$

Note that the radiance and BRF responsivity predictions and variances depend on the current value of Y. The last terms inside the radicals are the systematic uncertainties in the MODIS system, and are determined prelaunch.

9 Initialization

Before operational or SD calibration processing can begin there are a set of variables that must be available to the algorithm. Some of these variables are defined during the Activation and Evaluation (A&E) period, while others must be initialized from external tables or data statements. All necessary initialization variables are described here along with a procedure to obtain them.

9.1 Solar Spectral Irradiance

E_{sun} is needed to calculate SD spectral radiance for the radiance calibration (see Sections 4.5, and 6.1). The baseline procedure is to use the prelaunch radiance calibration as monitored by the SRCA during A&E, and is described in Guenther et al. [1995].

In order to utilize the SD as a radiance source, MODIS must either measure the solar irradiances in the solar reflective bands during a solar calibration period in A&E, or have access to a table of predefined solar irradiances. These irradiances must be stored in the table SOLAR_IRRAD for future access.

In the event that the prelaunch radiance calibration and the SRCA-derived calibration do not become available, then solar irradiance values computed in an off-line environment for the MODIS bands would be placed in the table SOLAR_IRRAD. The accepted relative spectral response functions of the MODIS filters in conjunction with the solar irradiance measurements compiled by Wehrli [1986] could serve as the source for the table. System-level calibration using NIST-traceable irradiance sources serves as another option for radiance calibration.

If the SRCA-monitored prelaunch MODIS radiance responsivities are used during A&E to calculate radiance, the calibration equation, if used for measuring SD radiance during a solar calibration period, is

$$L_{SD}(B,D,M,S) = \frac{\overline{DN}_{SD}(B,D,S)}{{}^{0}_{L}(B,D)}$$

where ${}^{0}_{L}(B,D)$ is the A&E radiance responsivity for detector D in band B, and we assume that ${}^{0}_{L}(B,D)$ applies to both scan-mirror sides; and $\overline{DN}_{SD}(B,D,S)$ is the average effective counts for scan S of the SD. Note that there is no distinction between scan-mirror sides in this development. The notation and arrays used here are similar in form to those in Section 6, except that the reference to mirror side is omitted. From Section 6.1 the theoretical SD radiance at each band, and scan is given by

$$L_{SD}(B,S) = R_T\ E_{sun}(B)\ \bar{\tau}_{SD}(S)\ \overline{BRDF}_{SD}(B,S)\ \cos(\theta_{SD})(S)$$

where we assume no dependence on detector, since the SD is a spatially uniform source of radiance, and that the SD degradation factor, Δ, is unity during A&E. Using the two equations above, the measured radiances are regressed on the theoretical radiances using a straight-line zero-intercept model, and $E_{sun}(B)$ is treated as the unknown proportionality constant to be estimated. However, since there is no explicit dependence of $E_{sun}(B)$ on detector, we arbitrarily choose the data from any detector within a band for the regression calculations. In matrix form

$$\mathbf{DN}_{SD}(B,D) = E_{sun}(B)\ \mathbf{Q}_{SD}(B,D) + \varepsilon$$

where the S^{th} component of the vector $\mathbf{Q}_{SD}(B,D)$ is

$$\left[\mathbf{Q}_{SD}(B,D)\right]_S = {}^{0}_{L}(B,D)\ R_T\ \bar{\tau}_{SD}(S)\ \overline{BRDF}_{SD}(B,S)\ \cos(\theta_{SD})(S),$$

and ε is a gaussian random vector with mean zero and variance σ_E^2. The input data are the measured average effective detector counts for detector D for each scan. Expressing the equation above in component form we have

$$\begin{bmatrix} \overline{DN}_{SD}(B,D,1) \\ \overline{DN}_{SD}(B,D,2) \\ \vdots \\ \overline{DN}_{SD}(B,D,K_E) \end{bmatrix} = \begin{bmatrix} [\mathbf{Q}_{SD}(B,D)]_1 \\ [\mathbf{Q}_{SD}(B,D)]_2 \\ \vdots \\ [\mathbf{Q}_{SD}(B,D)]_{K_E} \end{bmatrix} [E_{sun}(B)] + \begin{bmatrix} \varepsilon_1 \\ \varepsilon_2 \\ \vdots \\ \varepsilon_{K_E} \end{bmatrix}$$

Each column vector contains K_E elements, the number of scans of the SD which occurred during the solar calibration period. The least-squares estimate of the solar irradiance, $E_{sun}(B)$, in band B, given the input data are from detector D, is

$$E_{sun}(B) = \frac{\mathbf{Q}_{SD}^T(B,D)\,\mathbf{DN}_{SD}(B,D)}{\mathbf{Q}_{SD}^T(B,D)\,\mathbf{Q}_{SD}(B,D)}$$

where T denotes matrix transpose. The standard error of $E_{sun}(B)$ is

$$S_E(B) = \sqrt{\frac{\left(\mathbf{DN}_{SD}(B,D) - E_{sun}(B)\ \ \mathbf{Q}_{SD}(B,D)\right)^T \left(\mathbf{DN}_{SD}(B,D) - E_{sun}(B)\ \ \mathbf{Q}_{SD}(B,D)\right)}{K_E - 1}\left(\mathbf{Q}_{SD}^T(B,D)\mathbf{Q}_{SD}(B,D)\right)}$$

9.2 SD Principal Axes

Three vectors specified in the MODIS coordinate system are needed to unambiguously specify the direction of the Sun on the SD surface.

9.3 SD BRDF

A two-dimensional lookup-table will contain SD BRDF measurements. Section 5 assumes that the quantity $BRDF_{A\&E}$ exists, and is proportional to the SD BRDF at the bidirectional angles defined by the solar incident irradiance, and the SDSM view angle. $BRDF_{A\&E}$ is estimated during A&E using the identical procedure used to estimate BRDF in Section 5.3. However there is a limited range of solar azimuth available during A&E to perform a full characterization of $BRDF_{A\&E}$. The characterization is extended to the full range of potential solar incidence and azimuth angles by normalization of $BRDF_{A\&E}$ to the prelaunch SD BRDF which resides in the table SD_BRDF. The SD BRDF factor $BRDF_{A\&E}$, resides in the table BRDF_A&E.

9.4 SDSM Screen Normal

The SDSM screen normal must be specified as a unit vector in the MODIS coordinate system.

9.5 SD Screen Transmittance

A two dimensional lookup-table for SD screen transmittance resides in the table SD_SCREEN_T.

9.6 SDSM Screen Transmittance

A two dimensional lookup-table for SDSM screen transmittance resides in the table SDSM_SCREEN_T.

9.7 Scan Mirror Reflectivity

The MODIS scan mirror relative reflectivity is updated after every SD calibration event. It resides in the table MIRROR_REFL.

9.8 Vicarious Calibration Correction Factors

Calculation of the radiance and BRF in Section 8.1 require that the vicarious calibration correction factors to radiance responsivity and BRF calibration coefficient be available. These two quantities are band dependent. The radiance correction factors are in the array $F_{VC,L}(B)$ of Section 8.1 and reside in the table VC_RADIANCE. The corresponding BRF calibration coefficient correction factors are in the array $F_{VC,\rho}(B)$ of Section 8.1 and reside in the table VC_BRF.

9.9 Systematic Uncertainties

Calculation of the radiance and BRF uncertainties in Section 8.2 requires that the MODIS systematic uncertainties be available. These two quantities are band and detector dependent. The radiance systematic uncertainties are in the array $S_L^{sys}(B, D)$ of Section 8.2 and reside in the table SYS_RADIANCE. The BRF systematic uncertainties are in the array $S_\rho^{sys}(B, D)$ of Section 8.2 and reside in the table SYS_BRF.

9.10 Responsivity Record

The responsivity record contains the history of detector responsivity estimates made during SD calibration events. New values are appended after each SD illumination period. The responsivity record is in the table RESP_RECORD.

9.11 Statistical Tables

Confidence intervals computed in the algorithm need access to tabulated values of the F distribution and Dixon's "R10" distribution. These tables are F_TABLE, and R10_TABLE, respectively. The tabulated critical points in these tables must correspond to the selected values of the control variables RESP_REJECT_LEVEL, and DN_REJECT_LEVEL, respectively.

9.12 Physical Constants

Two constants needed for future application are:
Planck's Constant: 6.6260755e-34 J s
Boltzman's Constant: 1.380658e-23 J/K

9.13 Computed Constants

Machine precision may vary in the operational environment. Assume acos(x) is a math library function that computes the Arccosine of x. Then π=acos(-1d0).

10 L1B Calibration Output Products

The following products represent the L1B output for the solar reflective bands during operational processing. EV as well as SV count data are converted to radiance and BRF. Data output includes all bands (B) and corresponding detectors (D). The units of radiance are $\left[\mathrm{W\ m^{-2}\ sr^{-1}\ \mu m^{-1}}\right]$, and BRF is a unitless quantity.

Variable	Operational Processing Product	Sec.
$L_{EV}(B,D)$	EV radiance	8.1
$S_{EV,L}(B,D)$	Uncertainty of EV radiance	8.2
$[\rho_{EV}\cos(\theta_{EV})](B,D)$	EV BRF-(cosine zenith angle) product.	8.1
$S_{EV,\rho}(B,D)$	Uncertainty of EV BRF-(cosine zenith angle) product.	8.2
$DN_0(B,D,1)$	SV buffer mean.	2.6, 6.6
$S_0(B,D,1)$	SV buffer standard deviation.	2.7, 6.6
$K_0(B,D,1)$	Number of elements in all SV scan vectors of SV buffer.	2.5, 6.6
$MN_0^0(B,D,1)$	Minimum SV buffer value.	2.8,6.6
$MX_0^0(B,D,1)$	Maximum SV buffer value.	2.8,6.6
SV_MIN(B,D,1)	Minimum of unfiltered current SV scan.	2.1.1,6.6
SV_MAX(B,D,1)	Maximum of unfiltered current SV scan.	2.1.1,6.6

The following products represent the L1B output for the solar reflective bands when the moon appears in the SV port (lunar mode). The data are the result of applying the calibration equations for radiance and BRF to the SV counts for those detector IFOVs projected onto the lunar surface. Data output includes all bands (B) and corresponding detectors (D). The units of radiance are $\left[\mathrm{W\ m^{-2}\ sr^{-1}\ \mu m^{-1}}\right]$, and BRF is a unitless quantity.

Variable	SV Lunar Mode Processing Product	Sec.
$L_{SV}(B,D)$	SV radiance.	
$S_{SV,L}(B,D)$	Uncertainty of SV radiance.	
$[\rho_{SV}\cos(\theta_{SV})](B,D)$	SV BRF-(cosine zenith angle) product.	
$S_{SV,\rho}(B,D)$	Uncertainty of EV BRF.	

The following products represent the L1B output for the solar reflective bands during solar calibration periods when the MODIS detectors sample the SD.

Variable	SD Processing Product	Sec.
$DN_{SD}(B,D,M,F)$	SD counts: band B, detector D, mirror-side M, sample F.	3.1

The following products represent the L1B output for the solar reflective bands after solar calibration period processing is complete. The data are the results of trending the radiance responsivities based on the historical record. Data output includes all bands (B) and corresponding detectors (D). The units of radiance responsivity are $\left[\text{counts W}^{-1}\text{ m}^{2}\text{ sr }\mu\text{m}\right]$, and the units of reflectance calibration coefficient are $\left[\text{counts}\right]$.

Variable	Solar Calibration Processing Product	Sec.
$_{L}(B,D)$	Radiance responsivity.	6.6
$S_{L}(B,D)$	Standard error of $_{L}(B,D)$.	6 .6
$b_{0}(B, D)$	Intercept of radiance responsivity trend function.	7.1
$b_{1}(B, D)$	Slope of radiance responsivity trend function.	7.1
$_{\rho}(B,D)$	Reflectance calibration coefficient.	TBD
$S_{\rho}(B,D)$	Standard error of $_{\rho}(B,D)$.	TBD
$b_{0\rho}(B, D)$	Intercept of reflectance calibration coefficient trend function.	TBD
$b_{1\rho}(B, D)$	Slope of reflectance calibration coefficient trend function.	TBD

The following products represent the L1B output for the solar reflective bands after solar calibration period processing is complete. The data are the results of estimating the radiance responsivities and from them calculating the scan-mirror-side relative reflectance. Data output includes all bands (B). The scan-mirror-side relative reflectance is a unitless quantity.

Variable	Scan Mirror Reflectance Product	Sec.
R(B, M)	Mirror-side relative reflectance	6.4

Control Variables

A summary of the control variables used in the algorithm is presented in the following table along with suggested values:

Control Parameter	Description	Value
MAX_REJECT	Maximum number of outliers rejected in one sample.	4
FSV	SV sector starting sample number FSV + $N_{SV} \leq$ 15, 30, or 60.	1
SD_B_SIZE	Total number of SD scans.	100
SDSM_B_SIZE	Number of SDSM scan cycles in SD cal. period (> 20).	30
SV_B_SIZE	Number of scans in the SV buffer.	25
FSD	SD sector starting sample number FSD + $N_{SD} \leq$ 15, 30, or 60.	1
TOTAL_CAL	Total number of SD calibration periods in the mission.	100
DN_REJECT_LEVEL	Count data outlier test level for R10_TABLE table.	0.01
RESP_REJECT_LEVEL	Responsivity outlier test level for F_TABLE.	0.01

Data Tables

A summary of the lookup tables needed by the algorithm is presented in the following table along with the section where they occur:

Table	Description	Section
R10_TABLE	Critical points of Dixon's R10 statistic.	2
SOLAR_IRRAD	Solar irradiance band-integrated for MODIS bands 1-19, 26.	4, 5
SD_SCREEN_T	SD screen transmittance.	4, 5
SD_BRDF	Prelaunch SD BRDF.	4, 5
SDSM_SCREEN	Unit vector containing the SDSM screen normal.	4
BRDF_A&E	SDSM BRDF factor computed during A&E.	5
MIRROR_REFL	Relative reflectivity of scan mirror sides.	6
RESP_RECORD	Table containing responsivity records and SD_YEAR(t).	6, 7
F_TABLE	Percentage points of the F distribution.	7
VC_RADIANCE	Vicarious calibration coefficient correction for radiance.	8
VC_BRF	Vicarious calibration coefficient correction for reflectance.	8
SYS_RADIANCE	MODIS systematic uncertainties for radiance	8
SYS_BRF	MODIS systematic uncertainties for reflectance	8

Change Information

September 1995 - Rev. A

- Current algorithm (ATBD '94) does not compute exponential trend function correctly. Replaced exponential function with a linear function.
- Correction to the SD screen transmittance. Should be 0.085 (Init_SD_Info)
- Correction to the boolean initializations of which detectors are calibrated with screen up or screen down. See the following table (SD.h):

September 1995 - Rev B.

- Clarified which detectors are to be calibrated with the SD screen down
- Scan buffer dimension (S) added to SV statistics arrays in sec. 2.
- Added reference to Sun-Earth distance formula in sec. 3.3.
- Referenced two-phase regression algorithm for detecting linearity changes in responsivity trend.
- Corrected standard deviation formula in sec. 7.2.

October 1995 - Rev. C

- Fully described the outlier detection algorithm (see Section 2.2)
- Inserted a statement about wavelength shift correction to E_{sun} (sec 3.5)
- Separated the SV processing section from the SD processing section. The SV processing section now contains a full description of the outlier algorithm and the method of handling the SV buffer statistics.
- Segregated the two mirror sides to allow estimation of relative reflectivity.
- Separated responsivity estimation between mirror sides.
- Preceded each section with tables listing variables, arrays, control parameters, and external data tables.
- Inserted headings and a table of contents.

October 1995 - Rev. D

- Collected all data tables into one section and provided descriptions of each table.
- Collected all control parameters into one section and provided descriptions of each table.
- Inserted reference to algorithm for measuring the solar irradiances during A&E using the prelaunch calibration.
- Expanded the Output Products (section 10) to include names of the arrays used in the algorithm which contain the output data.
- Included both high and low gain outputs of bands 13/13' and 14/14'.
- Defined the terms *operational processing* and *solar calibration processing*. Described how the calculations for SV statistics depend on which of these types of processing is in place.

December 1995 - Rev. E

- Removed offset correction of the SD count data (see Section 6.2 in Rev. D), since the effective count algorithm [Jones, 1995] performs the offset correction.
- Adjusted indexing on SV and SV frames to reflect that only 15 frames (1 km IFOV) are "usable" in the SV and SD.
- Replaced the use of the symbol "G" with the symbol to denote responsivity.
- Added the MODIS systematic uncertainties (in quadrature) to the radiance and BRF unertainties.
- Included the vicarious calibration correction to the radiance and BRF output products.

December 1995 - Rev. F

- Added the output product tables (see Section 10) which include SV radiance/BRF, SD response, and trend function parameters.

- Added the algorithm for estimating the solar irradiance (Section 9.1).